## Supplementary Information

# Ultrafast, Scalable Laser Photothermal Synthesis and Writing of Uniformly-Dispersed Metal Nanoclusters in Polymer Films

Pankaj Ghildiyal(a), Yong Yang(b), Dylan J. Kline(b), Scott Holdren(a), Michael R. Zachariah(c) *

(a) Department of Chemistry and Biochemistry, University of Maryland, College Park, MD 20742.

(b) Department of Chemical and Biomolecular Engineering, University of Maryland, College Park, MD 20742.

(c) Department of Chemical and Environmental Engineering, University of California, Riverside, CA 92507.

### S1. Finite Element Simulation Details

Following heat capacity ($C_p$) and thermal conductivity (k) data[1–3] was used to solve for the heat transfer simulation:

$C_{p,\ \text{polyvinylalcohol}} = -57.669\ [\text{J/(kg K)}] + 5.1944\ [\text{J/(kg K}^2)]\text{x}T$ $\quad [273K \leq T \leq 300\ K]$

$C_{p,\ \text{polystyrene}} = -95.668\ [\text{J/(kg K)}] + 4.393\ [\text{J/(kg K}^2)]\text{x}T$ $\quad [273K \leq T \leq 373K]$

$= 740.25\ [\text{J/(kg K)}] + 2.934\ [\text{J/ (kg K}^2)]\text{x}T$ $\quad [T > 373K]$

$C_{p,\ \text{glass}} = 828\ [\text{J/(kg K)}] + 0.4418\ [\text{J/(kg K}^2)]T - 1.7186 \times 10^7\ [\text{J K/kg}]/T^2$

$k_{,\ \text{polyvinylalcohol}} = 0.35\ [\text{W/(m K)}]$

$k_{,\ \text{polystyrene}} = 0.1455\ [\text{W/(m K)}] + 1.0\text{x}10^{-6}\ [\text{W/(m K}^3)]\text{x}(T - 273.2\text{K})^2$ $\quad [273K \leq T \leq 416K]$

$= 0.1659\ [\text{W/(m K)}]$ $\quad [T > 416\ K]$

$k_{,\ \text{glass}} = 0.5053\ [\text{W/(m K)}] + 1.750\text{x}10^{-3}\ [\text{W/(m K}^2)]T$

A constant extrapolation was assumed outside the specified temperature ranges.

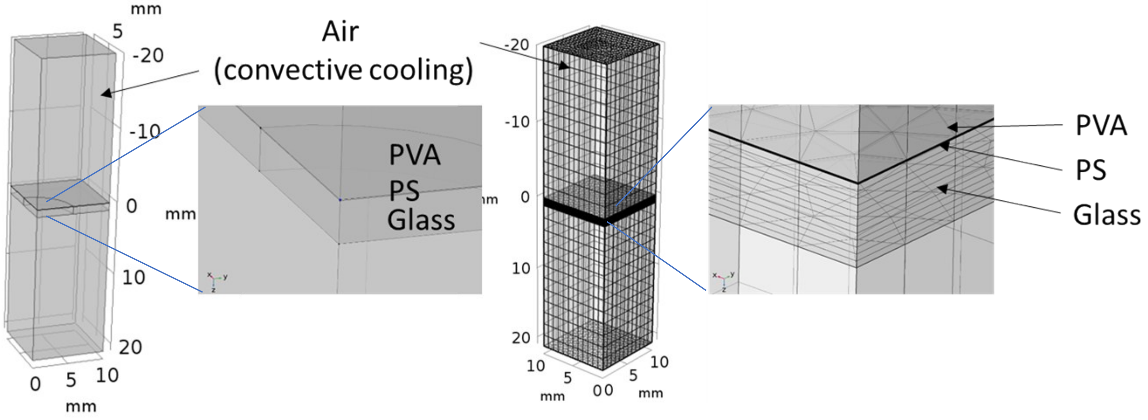

***Figure S1.*** *Model geometry (unmeshed and meshed) of laser heated system (PVA-PS-Glass) with the airbox for modeling of convective cooling. Constructed using COMSOL Multiphysics (version 5.3a****,*** *Build 275).*

A free triangular mesh of element size range 0.0082 mm-0.82 mm was generated in the topmost layer (PVA). Then, this mesh was then swept through the subsequent layers with the following element distribution along the vertical sweep axis:

PVA, PS, Glass: 10, 12, 12 elements per layer respectively.

For the airbox, 12 elements per box and a relatively coarser mesh was used to reduce the computational time. A point in the PVA film was used to probe heating rates and polymer temperature over time.

Following absorption coefficients (corrected to base e) were used in the ensuing model:

$\alpha$ (PVA) = 0.061 [$\mu m^{-1}$]

$\alpha$ (PS) = 0.01 [$\mu m^{-1}$]

$\alpha$ (silica glass) = 0.39 [$\mu m^{-1}$][4]

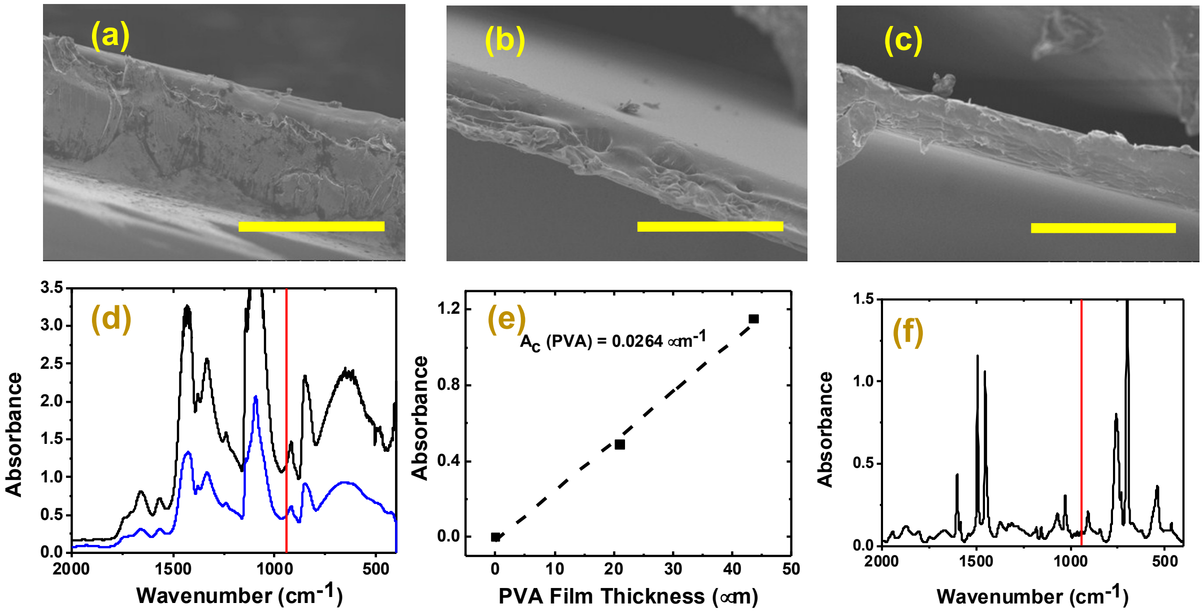

***Figure S2.*** *FESEM images of* ***(a)***, ***(b)*** *PVA films with different thickness,* ***(c)*** *PS film. Scale bars are 50*$\mu m$ *each.* ***(d)*** *FTIR-Transmission spectra of PVA films in (a) and (b).* ***(e)*** *Beer's law calibration curve and linear absorption coefficient at 10.6*$\mu m$, ***(f)*** *FTIR transmission spectra for PS film in (c). The solid red line denotes the operational* CO$_2$ *laser wavelength for LSPW.*

## S2. Selected Area Electron Diffraction Patterns and X-ray Diffraction Analysis of Metal-PVA films

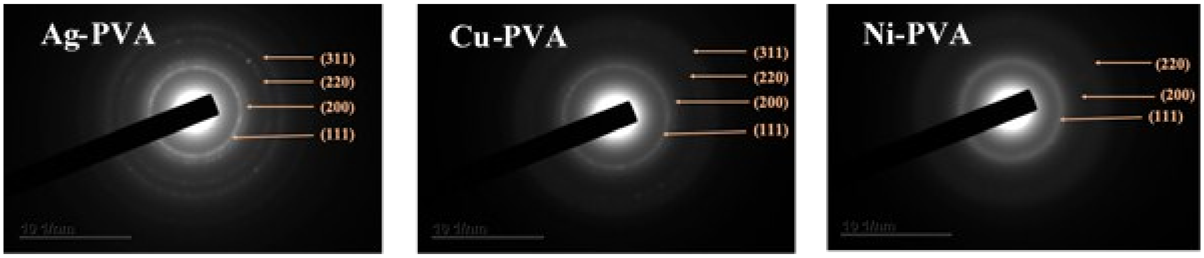

***Figure S3.*** *SAD patterns of Ag-PVA, Cu-PVA, and Ni-PVA fabricated by LSPW.*

In order to get reasonable XRD signals, we used thick polymer films with higher mass loadings of metals (metal:PVA = 0.6). Multiple laser spots (~8, 5 mm spot size) were written in the metal precursor-polymer film under appropriate reducing conditions. These films were scraped off and collected together to get a large enough quantity of the sample for XRD. We found that for metal-polymer (Ag-PVA) films prepared at shorter laser pulse durations, the XRD signal was extremely weak even for a large number of films. This may be due to the extremely small size of the nanoclusters (<10 nm), resulting in significant peak broadening.[5] In order to verify the crystallinity of the metals synthesized by laser heating and to confirm metal salt reduction (Cu and Ni, in particular), we therefore heated the films at a higher laser-energy flux and for a longer pulse duration to generate larger particles for sharper XRD signals. High metal loadings films under these conditions may generate larger, bulk metals in the polymer matrix. We obtained sharp metal peaks for Cu and Ni (face-centered cubic) with negligible or no oxide formation. This result corroborates the observations from TEM-Selected Area Diffraction patterns (Figure SX, Supplementary Information) and confirm that the metal salts have been reduced to the corresponding zero-valent metal nanoparticles in the presented laser approach.

The XRD spectra with the corresponding laser synthesis parameters are shown below**:**

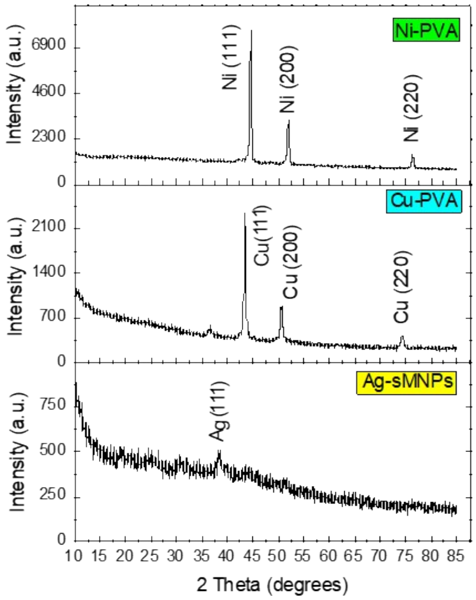

| Film | Metal:PVA mass ratio | Laser Energy Flux (W cm$^{-2}$) | Laser Spot Size (mm) | Laser Pulse Duration (ms) | Chamber Environment |
|---|---|---|---|---|---|
| Ag-PVA | 0.6 | 8 | 5 | 3000 | Ambient air |
| Cu-PVA | 0.6 | 10 | 5 | 5000 | 5% $H_2$ in $N_2$ |
| Ni-PVA | 0.6 | 10 | 5 | 7000 | 5% $H_2$ in $N_2$ |

All films were coated on 1 mm glass slides (polymer concentration: 0.75 g PVA in 5.5 mL $H_2O$, spin coated at (i) 250 rpm, 2s, (ii) 500 rpm, 10s.

***Figure S4.*** *XRD patterns of Ag-PVA, Cu-PVA, and Ni-PVA fabricated by LSPW.*

## S3: Number of Particles Counted for PSD Analyses

Figure 3

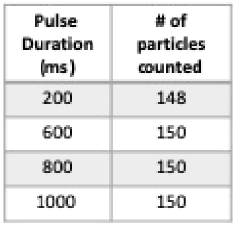

| Pulse Duration (ms) | # of particles counted |
|---|---|
| 200 | 148 |
| 600 | 150 |
| 800 | 150 |
| 1000 | 150 |

Figure 4

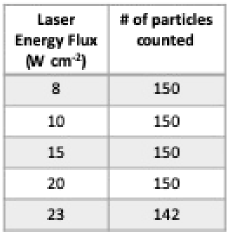

| Laser Energy Flux (W cm$^{-2}$) | # of particles counted |
|---|---|
| 8 | 150 |
| 10 | 150 |
| 15 | 150 |
| 20 | 150 |
| 23 | 142 |

Figure 5

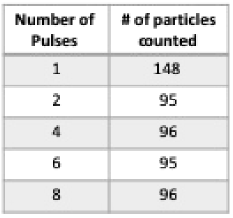

| Number of Pulses | # of particles counted |
|---|---|
| 1 | 148 |
| 2 | 95 |
| 4 | 96 |
| 6 | 95 |
| 8 | 96 |

Figure 6

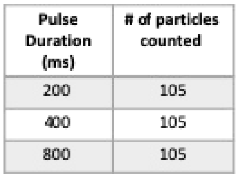

| Pulse Duration (ms) | # of particles counted |
|---|---|
| 200 | 105 |
| 400 | 105 |
| 800 | 105 |

## S4. Large Area TEM Images: Uniform Dispersions of Ag sMNPs

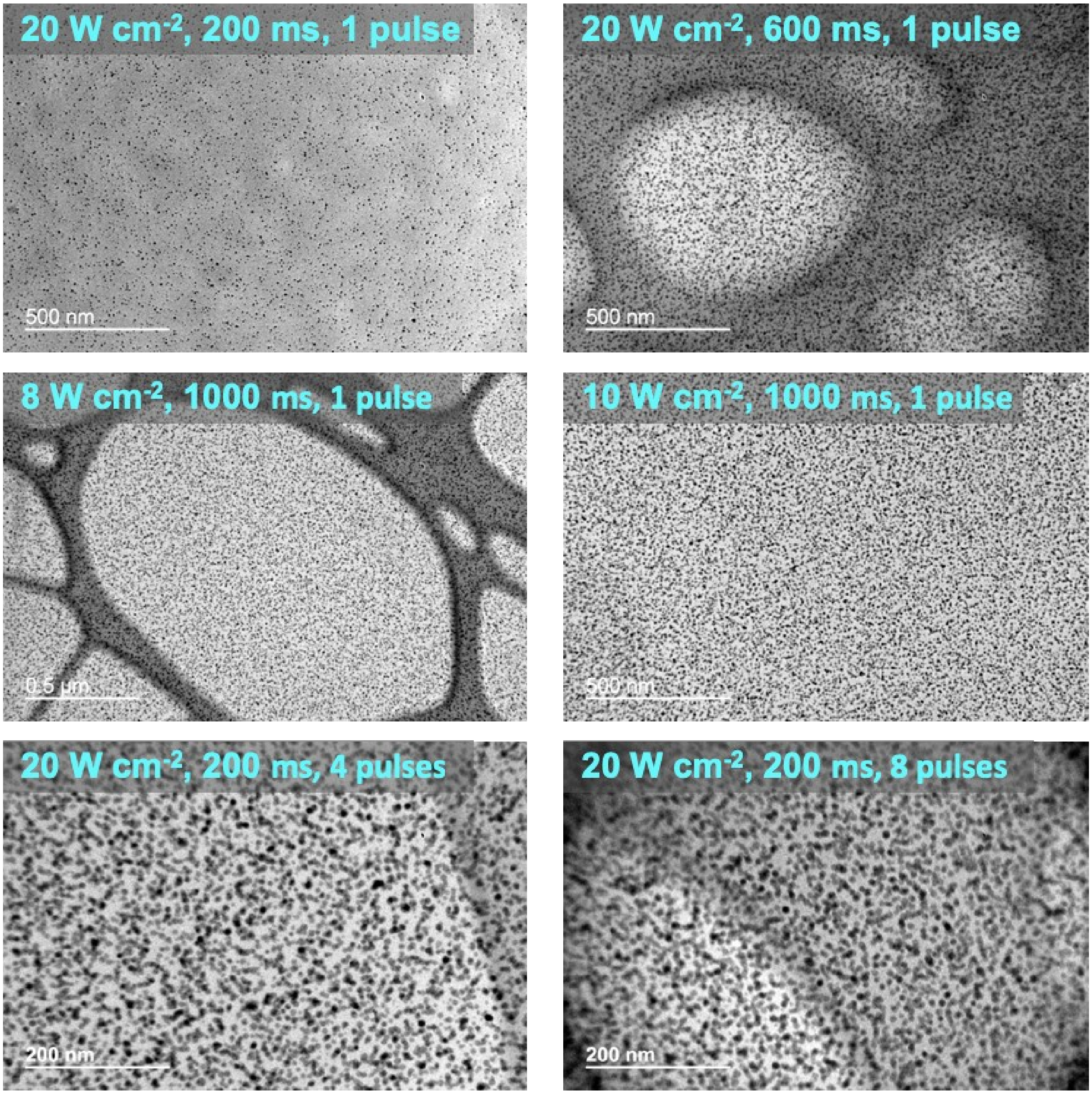

***Figure S5.*** *Large-area, low-magnification TEM images of Ag sMNP-PVA films fabricated with different laser heating characteristics. Substrate used is 1 mm glass.*

## S5. Effect of Substrate Characteristics

Here, we investigate the role of the underlying substrate, on which the aforementioned polymer films are coated. Since glass has the highest absorption coefficient in the mid-IR region, it can be assumed as a significant contributor to the thermal energy in the polymer films. Figure S5 shows Ag-PVA films fabricated using the same laser and polymer characteristics (89k PVA, 20 W $cm^{-2}$, 200ms) but on silica glass slides with different thicknesses (0.2 mm, and 1 mm). We see that particles are much bigger for films coated on a thinner glass slide (0.2 mm). A simple Beer's law calculation from absorption coefficient of glass shows that around 99% of the $CO_2$ laser energy is absorbed by only 12 μm of glass. This suggests that for a 0.2 mm slide, 6 % of the substrate depth acts as a heat-source, while the rest 94% acts as a heat sink. On the other hand, for a 1 mm slide, only 1% of the depth is heated and the 99% is responsible for conductive heat loss. Figure 8 (d) demonstrates that for a thinner glass substrate, the heat losses are limited and, thus, the heating rate and temperatures reached are much higher. This leads to formation of much larger particles for polymer films coated on a thin glass slide.

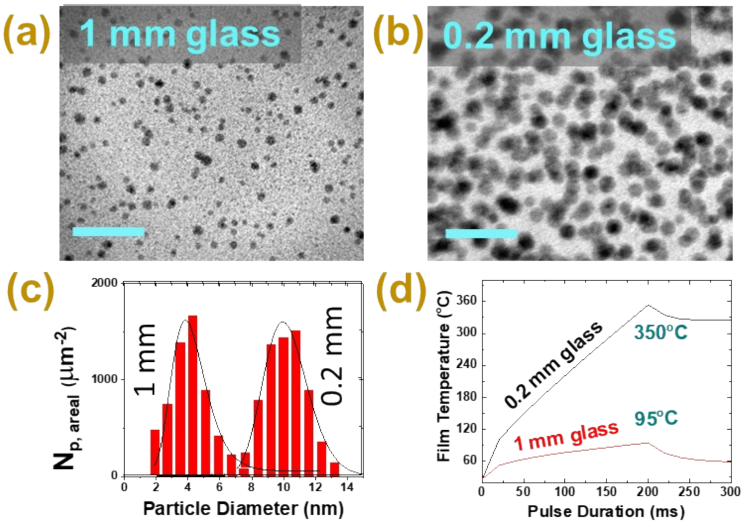

***Figure S6.*** ***(a), (b), (c)*** *TEM images (scale bar: 50 nm) and corresponding PSDs of Ag sMNPs films fabricated with a 20 W cm*$^{-2}$*, 200 ms pulse on different glass substrates,* ***(d)*** *Simulated laser heating profiles for the two glass substrates.*

Interestingly, we did not observe any particle formation for films coated on a silicon substrate, even for long pulse durations and high energy flux. Silicon with a much lower absorption coefficient than glass ($\alpha_{silicon} = 0.05\ \mu m^{-1} = 0.13\ \alpha_{glass}$). Not only does it not heat up itself, but also acts almost completely as a conductive heat sink for the thermal energy absorbed by the polymer films. In this case, the polymer films do not reach the required temperature as all incoming heat absorbed by the polymer films is lost quickly. The substrate, therefore, is crucial to the heat transfer processes in the polymer film.

## S6. Calculation of production rate

Laser spot diameter = 1 cm

Spot area = $\pi r^{2}_{laser}$= 3.14x10$^{-4}$ m$^2$

Freestanding PVA film thickness = 30 x 10$^{-6}$ m

Therefore, volume of the laser heated polymer spot = 9.42 x $10^{-8}$ $m^3$

Density of PVA = 1190 kg/$m^3$

Hence, mass of PVA = 1.50 x $10^{-5}$ kg

Mass ratio of Ag:PVA used to prepare the film = 0.05

Assuming complete conversion of $Ag^+$ to Ag,

Mass of Ag produced = 5.60 x $10^{-7}$ kg or 7.5 x $10^{-4}$ g

Laser heating pulse used to generate this amount of Ag = 35 ms

Considering the laser process to be continuous, we calculate:

Yield per minute = (5.6 x $10^{-4}$ g) x (60 s/min)/(0.035 s) = 0.96 g/min ~1 g/min

## S7. Lateral Heat Diffusion and Thermal Damage to Polymer Films in Laser Writing

We note that while the temperatures reached by laser heating are well-above the heat-proof temperature of PVA, the heating time is relatively shorter compared to the decomposition rate of the polymer. Reaction rates for thermal decomposition of PVA at similar temperatures have been calculated to be in the order of $10^{-3}$-$10^{-4}$ $s^{-1}$.[6] The timescales for half-decomposition of PVA must therefore be on the order of $10^3$-$10^4$ seconds, which is several orders of magnitudes slower than the fabrication timescales for laser heating (35-4000 milliseconds). Furthermore, in a previous study from our group[7], we observed (through FTIR analysis) that for short heating timescales (order of a few seconds), polymer degradation is minimal even for temperatures as high as 600°C. We, therefore, believe that polymer degradation and decomposition is not significant in our process. We have also been able to dissolve the polymer away and release the nanoclusters in water – the solvent for PVA, indicating that the polymer remains mostly intact during laser heating (shown in section S8, Supplementary Information). Although there may be some wrinkling/polymer damage in free-standing films, these damage effects may be reduced by using lower laser energy flux and/or pulsed heating technique as described in section 3.2.3.

For writing purposes, lateral heat diffusion during laser heating may limit the contrast in the patterns written in polymer substrates. Here, we discuss lateral thermal diffusion in polymer films during LSPW process. In laser heating experiments, we have observed that particle formation (indicated by the yellow coloration of Ag nanoparticles) occurred within the area defined by the laser beam spot size. The areas outside the written laser spot do not show significant coloration and particle formation. We investigated lateral heat diffusion by conducting finite-element simulations for laser heating (10 W $cm^{-2}$, 35 ms) of a free-standing 35 μm thick PVA film (Figure S7 (a) below).

Figure S7 (b) shows temperature profile of the film with increasing distance from the center of the laser beam spot (D_laser_center). We observe that the lateral heat diffusion in the polymer film is minimal during laser heating, as most of the heat is confined within the laser beam radius (T~220$^{o}$C within laser heated spot). Due to extremely low thermal conductivities of polymers (~0.1-0.3 W/(m K)), we believe that lateral heat diffusion is greatly suppressed. Although conductive quenching does occur laterally once the laser beam is turned off, the temperatures reached are much lower than the relevant temperatures required for metal nanocluster formation (<80$^{o}$C) and hence may not be significant in writing metal patterns. Lateral heat diffusion may further be attenuated by delivering the required thermal energy in the form of multiple short laser thermal pulses (as described in section 3.2.3).

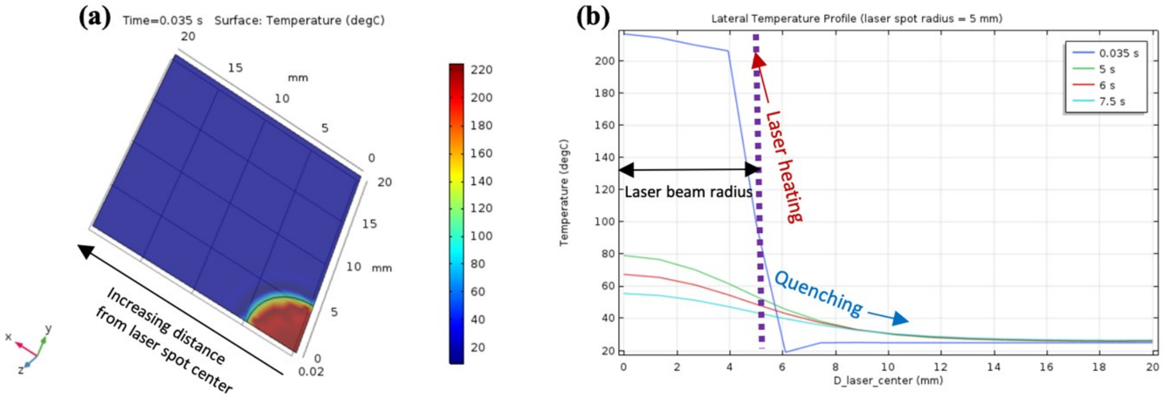

***Figure S7.*** ***(a)*** *Simulated laser heating of a freestanding PVA film,* ***(b)*** *Lateral temperature profile with increasing distance from the center of the laser beam spot during laser heating and quenching.*

## S8. Dispersibility of Laser-Written Metal Nanocluster-Polymer Films in Solutions

We found that laser written metal nanoclusters can be released into solutions by dissolving the polymer away. Multiple spots were written in the polymer film, after which Ag-PVA films were peeled off and dissolved in water at ~50$^o$C. After polymer film dissolution, the solution turned yellow (as shown in Figure (a) below) – due to the plasmonic absorption of laser written Ag particles released into the solution. Films that were not laser heated (no Ag nanoclusters) did not produce any color change when dissolved in water. We confirmed the dispersion of Ag NPs in water through visible absorption spectroscopy as shown below:

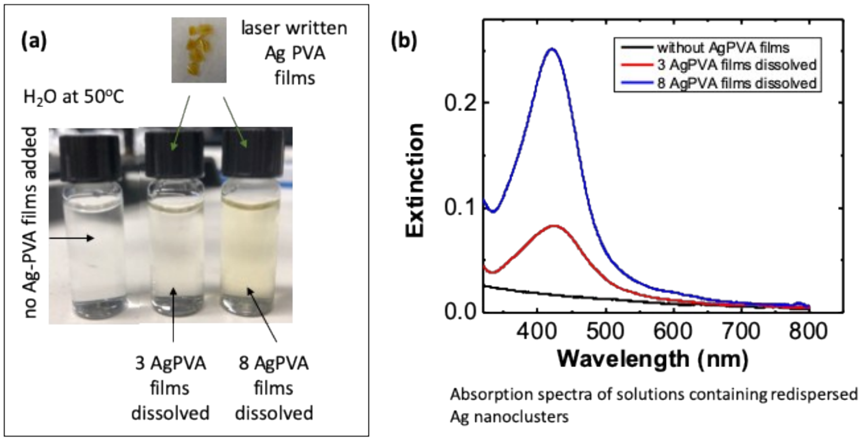

Absorption spectra of solutions containing redispersed Ag nanoclusters

***Figure S8.*** *Images and absorption spectra of solutions with laser written Ag-PVA films dissolved.*

**References:**

1 R. Kappes, F. Schönfeld, C. Li, A. Golriz, M. Nagel, T. Lippert, H. Butt and J. Gutmann, *Springerplus*, 2014, **3**, 489–489.

2 X. Xie, D. Li, T.-H. Tsai, J. Liu, P. V. Braun and D. G. Cahill, *Macromolecules*, 2016, **49**, 972–978.

3 U. Gaur, B. B. Wunderlich and B. Wunderlich, *J. Phys. Chem. Ref. Data*, 1983, **12**, 29–63.

4 N. Sahba and T. J. Rockett, *J. Am. Ceram. Soc.*, 1992, **75**, 209–212.

5 P. Scherrer, *Kolloidchem. Ein Lehrb.*, 1918, **2**, 387–409.

6 J.-L. Shie, Y.-H. Chen, C.-Y. Chang, J.-P. Lin, D.-J. Lee and C.-H. Wu, *Energy Fuels*, 2002, **16**, 109–118.

7 Y. Yang, M. Romano, G. Feng, X. Wang, T. Wu, S. Holdren and M. R. Zachariah, *Langmuir*, 2018, **34**, 585–594.